

# Glacial to Holocene swings of the Australian–Indonesian monsoon

Mahyar Mohtadi<sup>1\*</sup>, Delia W. Oppo<sup>2</sup>, Stephan Steinke<sup>1</sup>, Jan-Berend W. Stuut<sup>1,3</sup>,  
Ricardo De Pol-Holz<sup>4,5</sup>, Dierk Hebbeln<sup>1</sup> and Andreas Lückge<sup>6</sup>

**The Australian–Indonesian monsoon is an important component of the climate system in the tropical Indo-Pacific region<sup>1</sup>. However, its past variability, relation with northern and southern high-latitude climate and connection to the other Asian monsoon systems are poorly understood. Here we present high-resolution records of monsoon-controlled austral winter upwelling during the past 22,000 years, based on planktic foraminiferal oxygen isotopes and faunal composition in a sedimentary archive collected offshore southern Java. We show that glacial–interglacial variations in the Australian–Indonesian winter monsoon were in phase with the Indian summer monsoon system, consistent with their modern linkage through cross-equatorial surface winds. Likewise, millennial-scale variability of upwelling shares similar sign and timing with upwelling variability in the Arabian Sea. On the basis of element composition and grain-size distribution as precipitation-sensitive proxies in the same archive, we infer that (austral) summer monsoon rainfall was highest during the Bölling–Allerød period and the past 2,500 years. Our results indicate drier conditions during Heinrich Stadial 1 due to a southward shift of summer rainfall and a relatively weak Hadley cell south of the Equator. We suggest that the Australian–Indonesian summer and winter monsoon variability were closely linked to summer insolation and abrupt climate changes in the northern hemisphere.**

The seasonality of the global monsoon is of central importance to the global hydrologic cycle and its environmental influence on human societies. Palaeoclimate reconstructions generally agree that the strengths of the East Asian monsoon and the Indian monsoon are tightly coupled to the Northern Hemisphere climate through zonal migrations of the monsoon convection centres, also interpreted as Intertropical Convergence Zone (ITCZ) migration<sup>2–6</sup>. The mechanism of the Australian–Indonesian monsoon (AIM) in both time and space is, however, poorly understood<sup>7–12</sup>. Australian records<sup>9–11</sup> indicate wetter-than-today conditions during the early and middle Holocene. These changes have been explained through a Northern Hemisphere insolation control on the AIM (refs 8, 10), regional sea-surface-temperature (SST) feedback<sup>7</sup> or human impact on the late Holocene vegetation cover<sup>8</sup>, countering or even cancelling the response of the AIM to local insolation. Deglacial sea-level rise and its effect on exposed land surface may also be an important influence on southeast Indonesian rainfall<sup>12,13</sup>. Moreover, many records suggest that the Asian monsoons, including the AIM, changed in association with North Atlantic deglacial climate

oscillations that were accompanied by variations in the Atlantic Meridional Overturning Circulation (AMOC; refs 3,10,14). Further records of the AIM, especially those that reflect a known season, are needed to understand how these various possible influences affect the AIM.

Here we present high-resolution palaeoclimatic records from sediment core GeoB 10053-7 collected off South Java (8° 41' S, 112° 52' E, 1,375 m water depth, Fig. 1) that span the past 22,000 years. At present, the seasonal migration of the coupled monsoon–ITCZ systems governs the seasonal climate variability at the core site. During austral summer (henceforth summer), the northwest monsoon gathers large amounts of moisture while crossing sea from the Asian high-pressure belt on its way to the ITCZ. Maximum rainfall reaches the study area, including eastern Indonesia and Australia, in January (Fig. 1). During austral winter (henceforth winter), the southeast monsoon originates from the Southern Hemisphere high-pressure belt and the study area is relatively dry and cool. Ekman transport and coastal upwelling in the study area peak between July and September (see Supplementary Information).

Our palaeoclimate time series resolve both seasonal signals of the AIM in the same, continuous sedimentary archive over the past 22,000 years. We use *Globigerina bulloides* percentages as a proxy for winter upwelling and monsoon intensity. Our results suggest that upwelling off Java, and thus the Australian–Indonesian winter monsoon (AIWM), was weakest during the Last Glacial Maximum (LGM) and the late Holocene, and strongest during the early Holocene. These trends are paralleled by trends in the difference in  $\delta^{18}\text{O}$  of calcite between the annual-mean and winter ( $\Delta\delta^{18}\text{O}$ ), whereby greater differences imply stronger upwelling and intensified AIWM (Fig. 2c, see Supplementary Information). Differences between these upwelling-sensitive records are probably due to the additional and different influences of temperature on the individual  $\delta^{18}\text{O}$  records. Similar upwelling trends in the Arabian Sea<sup>14</sup> (Fig. 2e) during the same season (that is boreal summer and austral winter) indicate that these upwelling systems changed together, and provide strong evidence that they reflect variations in the strength of large-scale cross-equatorial boreal summer–austral winter monsoon winds, probably in response to Northern Hemisphere summer insolation<sup>7,15</sup> (Fig. 2d). This inference should be explored further with AIWM records that span several glacial–interglacial cycles.

Superimposed on the long-term variability of the Java upwelling are a number of deglacial AIWM variations of millennial-scale

<sup>1</sup>Center for Marine Environmental Sciences (MARUM), University of Bremen, 28359 Bremen, Germany, <sup>2</sup>Geology & Geophysics, Woods Hole Oceanographic Institution (WHOI), Woods Hole, Massachusetts 02543, USA, <sup>3</sup>Royal Netherlands Institute for Sea Research (NIOZ), NL-1790 AB, Texel, The Netherlands, <sup>4</sup>Earth System Science Department, University of California, Irvine, California 92697, USA, <sup>5</sup>Department of Oceanography, Universidad de Concepción, Concepción, Chile, <sup>6</sup>Federal Institute for Geosciences and Natural Resources (BGR), 30655 Hannover, Germany.

\*e-mail: mohtadi@uni-bremen.de.

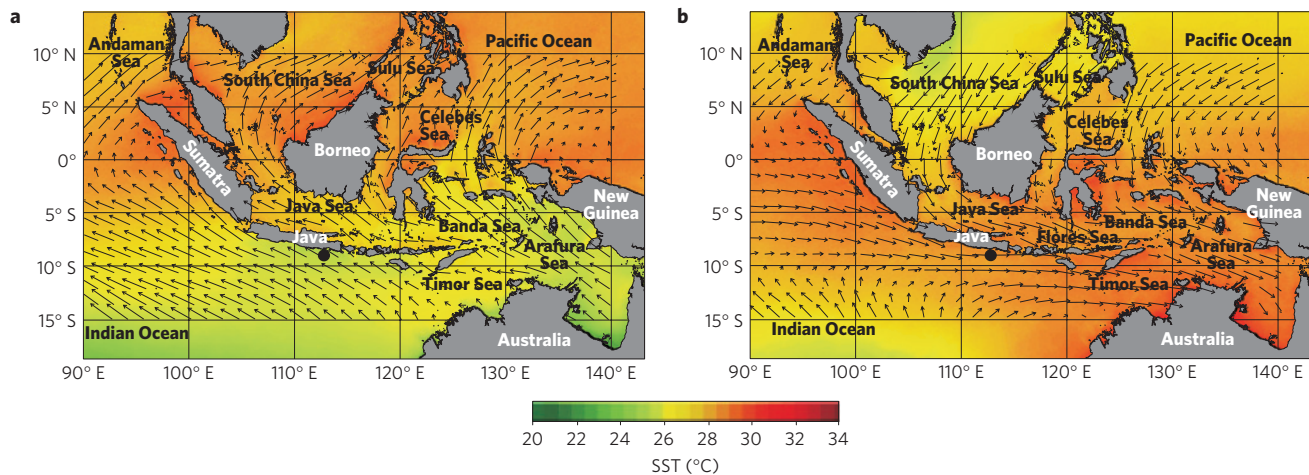


**Figure 1 | Monsoonal cyclicality in SST and wind trajectory in the tropical Indo-Pacific.** **a,b**, The colour chart indicates seasonal SSTs for winter (**a**, July–September) and summer (**b**, January–March). Remote-sensing SST data are averaged from January 2002 to February 2008 (Aqua MODIS, <http://oceancolor.gsfc.nasa.gov>). Superimposed are quick scatterometer winds (arrows) in August (**a**) and February (**b**; ref. 24). Wind data are averaged from December 1997 to June 2004 and from July 1999 to January 2005, respectively. The black circle indicates the position of the investigated core.

duration, that are best expressed in the percentage of *G. bulloides*. Although these variations are relatively subtle, similar features are recorded in the upwelling record from the Arabian Sea<sup>14</sup>, suggesting that they reflect large-scale changes in southerly cross-equatorial winds. For example, the relative contributions of *G. bulloides* of both regions (Fig. 2d,e) suggest modestly higher upwelling during the Heinrich Stadial 1 period (HS 1) that deteriorated to near glacial values during the Bölling–Allerød period (B–A), followed by intensified upwelling during the Younger Dryas period (YD). The coincident timing of the observed millennial-scale oscillations in the upwelling area off South Java and the Arabian Sea during the last deglaciation indicates that changes in the AIWM intensity were closely linked to the Indian monsoon. Moreover, these millennial oscillations are closely related to abrupt climate changes in the North Atlantic region (Fig. 2a). We note that a significantly larger surface reservoir age than used here (see Supplementary Information) might align these abrupt events better with North Atlantic events. A better alignment of these events with the onset of Southern Hemisphere climate at 18,000 years ago (for example Fig. 2g) and the end of the Antarctic Cold Reversal would require a less-than-zero surface-reservoir age.

Proxy records for runoff also enable us to evaluate changes in the Australian–Indonesian summer monsoon (AISM). In contrast to the AIWM, there is little evidence for large LGM–Holocene trends in AISM, with only Ti/Ca ratios suggesting that the Holocene was slightly wetter than the LGM and early deglacial (HS 1). This trend, although small, is consistent with the opposite evolution of the boreal winter monsoon in the Northern Hemisphere<sup>16</sup>, as recorded in Chinese loess sediments (Fig. 3e). Instead, millennial-scale oscillations dominate the records. The terrigenous fraction of the sediment indicates higher continental runoff caused by stronger AISM rainfall during the B–A and the past 2,500 years (Fig. 3b–c). In contrast, the LGM, HS 1 and YD are characterized by the lowest continental runoff due to a less intense AISM. The grain-size distribution of the terrigenous fraction in 112 selected samples further supports these findings (Fig. 3d, Supplementary Information). Sediments deposited during the HS 1 and YD are characterized by a lower terrigenous content that is coarser than during the remaining periods, suggesting a predominantly eolian source of the terrigenous sediment fraction, possibly transported from the interior of Australia. Conversely, sediments deposited during the B–A and the late Holocene contain more fine terrigenous components, suggestive of increased continental runoff and a

dominant fluvial source of the terrigenous fraction due to increased AISM rainfall. In summary, our proxy data from south of Java show a strong (wet) AISM during the B–A and the late Holocene, and a weak (dry) AISM during HS 1 and the YD, indicating that the AISM intensity was also closely linked to the Northern Hemisphere abrupt climate changes during the last deglaciation (Fig. 3a–c).

Our inferences of AISM and AIWM millennial variability are not entirely consistent with the interpretation of speleothem  $\delta^{18}\text{O}$  records from the East Asian monsoon and AIM regions, which may vary owing to a number of processes<sup>17,18</sup>. Chinese speleothem records have generally been interpreted to reflect changes in the relative strengths of the East Asian boreal summer and winter monsoon (EAWM and EASM) intensities, and suggest a relatively weak EASM during HS 1 and the YD and a relatively strong EASM during the B–A (ref. 3; Fig. 2f). The opposite developments of the AIWM and EASM during these periods (Fig. 2) is surprising, given that the AIWM winds at present ‘feed’ the EASM through cross-equatorial winds (Fig. 1). It is possible that millennial-scale variations in the  $\delta^{18}\text{O}$  of precipitation over coastal China reflect changes in the source of precipitation and the influence of upwind hydrologic non-local changes in the amount effect, as suggested by recent modelling studies<sup>18</sup>, and these changes are decoupled from cross-equatorial winds.

Our sedimentary evidence of AISM variability, suggesting drier conditions during HS 1 and wetter conditions during most of the B–A, are consistent with speleothem  $\delta^{18}\text{O}$  records from northwestern Borneo<sup>13</sup> (Fig. 3f). Together with records from Lynch’s Crater in northeastern Australia, which show increased moisture during HS 1 (refs 19,20), they suggest a southerly position of the austral summer ITCZ compared with the present. Although drying during HS 1 inferred from our records and the Borneo  $\delta^{18}\text{O}$  record is consistent with a large decrease in local rainfall during dramatic AMOC events such as HS 1 (ref. 18), the evidence for the YD is more complex. Whereas our records suggest a weaker AISM (drying) during the YD, speleothem records from both Borneo and Flores<sup>12</sup> imply a return to wetter conditions during the YD (Fig. 3f,g). These differences may imply that the mechanisms causing  $\delta^{18}\text{O}$  changes in precipitation of the region are more complex during times of modest AMOC reduction, or that there were sharp northeast-to-southwest gradients in precipitation within Indonesia. Simulations of the rainfall variability over the Indo-Pacific Warm Pool suggest an eastward displacement of the Walker and Hadley Circulations during the LGM (ref. 21),

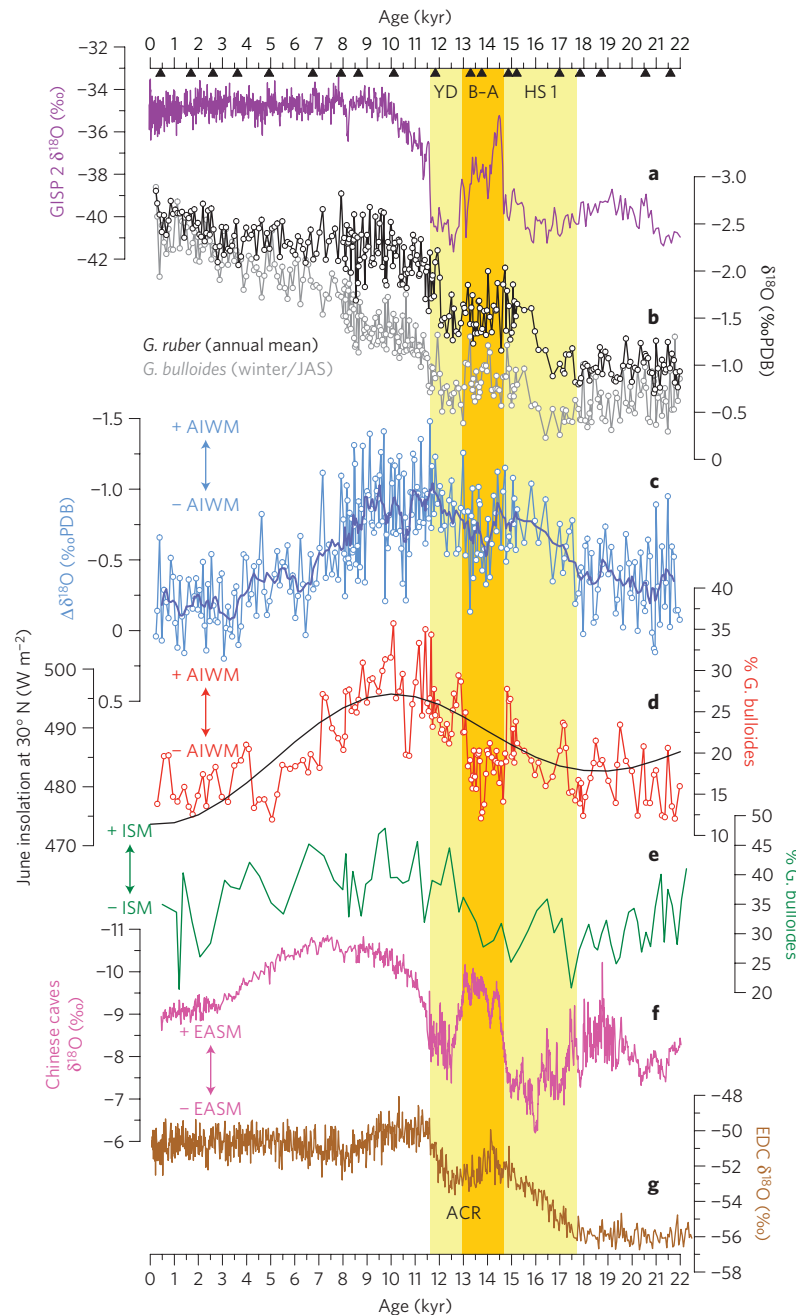


**Figure 2 | Proxy records for the winter AIM and other palaeoclimate records over the past 22,000 years.** **a**,  $\delta^{18}\text{O}$  record of GISP 2 ice core (Greenland)<sup>25</sup>. **b**,  $\delta^{18}\text{O}$  records of *Globigerinoides ruber* (black, annual mean) and *G. bulloides* (grey, winter, July–September) in core Geob 10053-7 off southern Java. **c**, Their difference ( $\Delta\delta^{18}\text{O}$ , blue), with a nine-point running average (thick dark-blue line). **d**, Relative contribution of *G. bulloides* (red) in the same core; superimposed is the June insolation at 30° N (black). **c** and **d** indicate changes in the upwelling intensity off southern Java that is controlled by the AIWM. **e**, Relative contribution of *G. bulloides* (green) in the Arabian Sea<sup>14</sup> indicative of changes in the Indian Summer Monsoon (ISM). **f**, Stacked  $\delta^{18}\text{O}$  of stalagmites in Chinese caves<sup>26</sup> (pink) indicating changes in the EASM-related precipitation. **g**,  $\delta^{18}\text{O}$  record of EPICA Dome C (EDC) ice core (East Antarctica, brown)<sup>27</sup>. Triangles denote radiocarbon datings; vertical bars correspond to the HS 1, B-A and YD periods, respectively. ACR, Antarctic Cold Reversal.

and a weakened and easterly displaced Hadley Circulation in the southern part of the Indo-Pacific Warm Pool during HS 1 and the YD in response to a weak AMOC (ref. 22). Although boundary conditions during the LGM and deglaciation were not considered in these simulations, these results suggest that weaker and easterly displaced convection centres might have caused the dry conditions observed in our proxy records during the LGM, HS 1 and YD. It should be noted that the timing of deglacial millennial-scale variability discussed above is subject to

uncertainties in our age model (as discussed in Supplementary Information). Although future work in the Java upwelling area should attempt to describe reservoir age changes through time, it is unlikely that age discrepancies alone account for differences in interpretation between our records and the published speleothem records from this region.

The Holocene evolution of the AISM rainfall in our records, a drier early and middle Holocene compared with the late Holocene (Fig. 3), differs from evidence from the Indo-Pacific

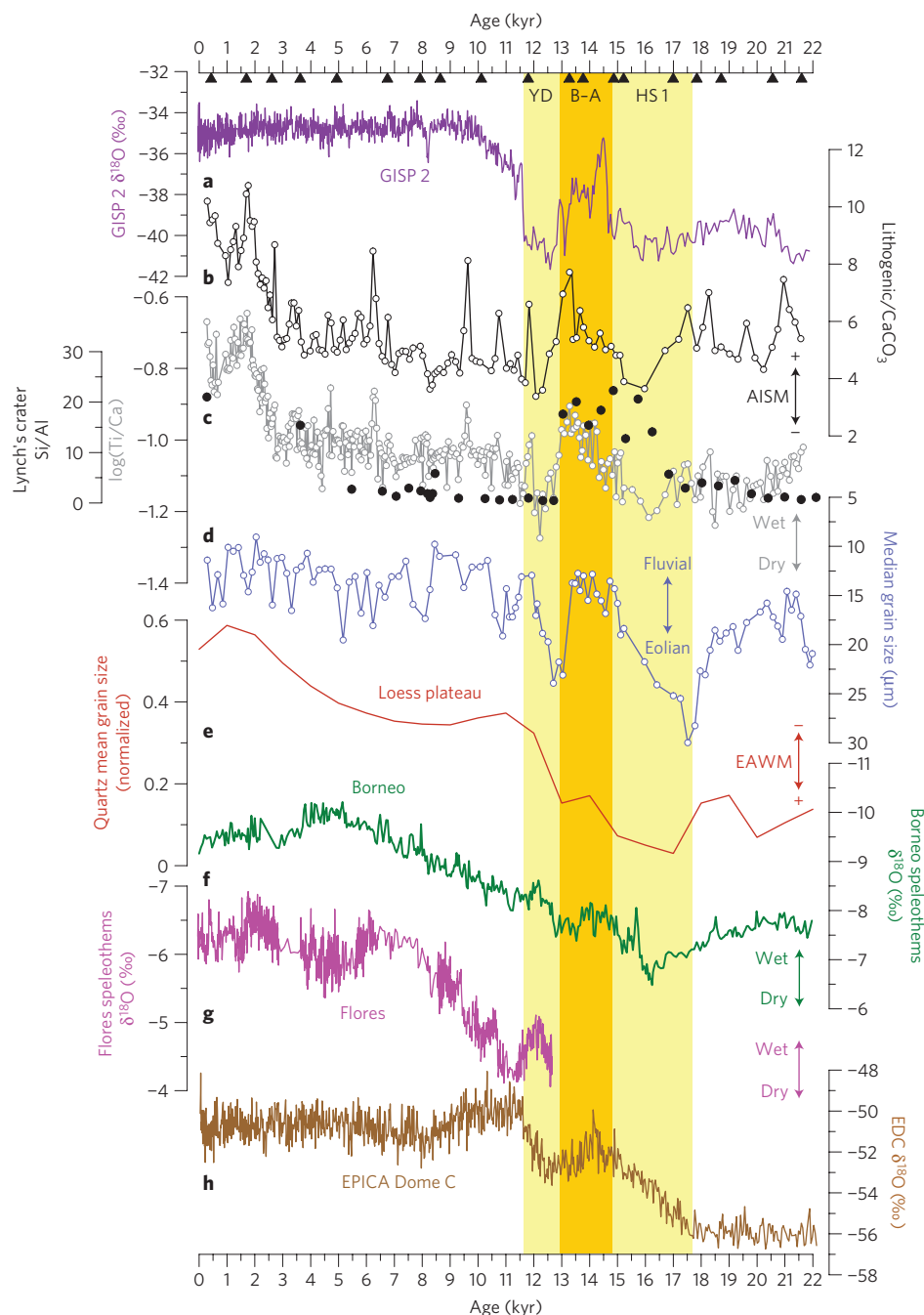


**Figure 3 | Proxy records for the summer AIM and other palaeoclimate records over the past 22,000 years.** **a**,  $\delta^{18}\text{O}$  record of GISP 2 ice core (Greenland)<sup>25</sup>. **b, c**, Lithogenic/CaCO<sub>3</sub> (**b**, black) and Ti/Ca (**c**, grey) ratios in core GeoB 10053-7 off southern Java. Superimposed are Si/Al data (black dots) from Lynch's Crater<sup>20</sup>. **d**, Median grain size of the terrigenous fraction of the sediment (blue). **b-d** indicate changes in the amount (**b, c**) and composition (**d**) of the continental runoff that is controlled by the AISM. **e**, Stacked mean grain size of quartz in the Chinese Loess Plateau<sup>16</sup> (red), indicative of changes in the EAWM intensity. **f**, Stacked  $\delta^{18}\text{O}$  of speleothems in Borneo<sup>13</sup> (green). **g**, Stacked  $\delta^{18}\text{O}$  of speleothems in Flores<sup>12</sup> (pink), indicating changes in the AISM- and sea-level-related precipitation. **h**,  $\delta^{18}\text{O}$  record of EPICA Dome C (EDC) ice core (East Antarctica, brown)<sup>27</sup>. Vertical bars, triangles and abbreviations are as in Fig. 2.

Warm Pool records, whereas Australian lake sediments<sup>9–11</sup> indicate conditions wetter than today during the early and middle Holocene. One possible explanation for the difference in timing between Australia and Flores/Java is the northward shift of austral summer precipitation (ITCZ). In this scenario, the earlier maximum in Borneo than Flores/Java may be because it reflects both summer and winter precipitation<sup>12</sup>. Alternative explanations for the different trends include changes in boundary conditions over the Australian landmass<sup>7,8</sup>. More data and modelling experiments

are needed to identify the most important mechanisms for these different trends.

Our results clearly indicate similar long-term variations of the AIWM wind and the EASM rainfall, probably due to their common forcing by Northern Hemisphere summer insolation. Glacial–interglacial AISM rainfall changes are small, but negatively correlated to the EAWM, as expected from north-to-south ITCZ migrations. On millennial timescales, however, variations in AIWM winds are not in agreement with interpretations of

Chinese speleothem  $\delta^{18}\text{O}$  records as reflecting variations in the seasonality of precipitation, consistent with modelling evidence that the  $\delta^{18}\text{O}$  of East Asian monsoon precipitation in response to abrupt AMOC events is controlled by other mechanisms, which will have to be explored further in future studies. Our results confirm a spatially coherent drying pattern throughout Indonesia due to southerly displaced ITCZ during the strong AMOC reduction of HS 1. However, our evidence of reduced runoff during the YD contrasts with Indonesian speleothem evidence of wetter conditions, suggesting either that mechanisms other than enhanced rainfall influenced speleothem  $\delta^{18}\text{O}$ , or that there were sharp precipitation gradients in Indonesia at this time. Sediment-age model uncertainties, which may lead to some of these discrepancies on millennial timescales, will also have to be explored in future studies.

## Methods

The age model is based on 19 radiocarbon dates yielding average sedimentation rates of  $37 \text{ cm kyr}^{-1}$  (see Supplementary Information). We analysed the stable oxygen isotope ( $\delta^{18}\text{O}$ ) composition in calcite shells of the surface-dwelling planktonic foraminifera *G. ruber sensu stricto* and *G. bulloides* in 290 samples, achieving an average temporal resolution of 75 years per sample. Modern observations from the study area show that *G. ruber* reflects annual-mean surface conditions, whereas *G. bulloides* records surface conditions during the winter AIM (ref. 23; AIWM, June–October), when coastal upwelling occurs (see Supplementary Information). We calculated the abundance of *G. bulloides* relative to total planktonic foraminiferal fauna as a measure of past changes in upwelling intensity. In this context, higher values of *G. bulloides* are interpreted as intensified upwelling caused by a stronger winter monsoon.

We also carried out element analyses using the X-ray fluorescence method, and calculated the lithogenic fraction of sediment. Variations in the Ti/Ca ratio determined by X-ray fluorescence and in the lithogenic/CaCO<sub>3</sub> ratio from the bulk sediment analysis show a strong correlation throughout the entire record (Fig. 3). On the basis of modern observations, these ratios represent continental runoff that is controlled by the summer AIM (AISM, December–March) precipitation, with higher ratios reflecting enhanced runoff and a stronger AISM (see Supplementary Information). Median grain size, measured with a laser particle sizer, provides a qualitative measure for the source of the terrigenous components, with smaller size indicating more fluvial delivery and larger sizes indicating more eolian delivery.

Received 26 January 2010; accepted 17 June 2011; published online 24 July 2011

## References

1. Webster, P. J. *et al.* Monsoons: Processes, predictability, and the prospects for prediction. *J. Geophys. Res.* **103**, 14451–14510 (1998).
2. Wang, Y. *et al.* The Holocene Asian monsoon: Links to solar changes and North Atlantic Climate. *Science* **308**, 854–857 (2005).
3. Wang, Y. J. *et al.* A high-resolution absolute-dated Late Pleistocene monsoon record from Hulu Cave, China. *Science* **294**, 2345–2348 (2001).
4. Chao, W. C. & Chen, B. The origin of monsoons. *J. Atmos. Sci.* **58**, 3497–3507 (2001).
5. Wang, P. Global monsoon in a geological perspective. *Chin. Sci. Bull.* **54**, 1113–1136 (2009).
6. Gupta, A. K., Anderson, D. M. & Overpeck, J. T. Abrupt changes in the Asian southwest monsoon during the Holocene and their links to the North Atlantic Ocean. *Nature* **421**, 354–357 (2003).
7. Liu, Z., Otto-Bliesner, B., Kutzbach, J., Li, L. & Shields, C. Coupled climate simulation of the evolution of global monsoons in the Holocene. *J. Clim.* **16**, 2472–2490 (2003).
8. Miller, G. *et al.* Sensitivity of the Australian Monsoon to insolation and vegetation: Implications for human impact on continental moisture balance. *Geology* **33**, 65–68 (2005).
9. Johnson, B. J. *et al.* 65,000 years of vegetation change in central Australia and the Australian summer monsoon. *Science* **284**, 1150–1152 (1999).

10. Magee, J. W., Miller, G. H., Spooner, N. A. & Questiaux, D. Continuous 150 k.y. monsoon record from Lake Eyre, Australia: Insolation-forcing implications and unexpected Holocene failure. *Geology* **32**, 885–888 (2004).
11. Nott, J. & Price, D. Plunge pools and paleoprecipitation. *Geology* **22**, 1047–1050 (1994).
12. Griffiths, M. L. *et al.* Increasing Australian–Indonesian monsoon rainfall linked to early Holocene sea-level rise. *Nature Geosci.* **2**, 636–639 (2009).
13. Partin, J. W., Cobb, K. M., Adkins, J. F., Clark, B. & Fernandez, D. P. Millennial-scale trends in west Pacific warm pool hydrology since the Last Glacial Maximum. *Nature* **449**, 452–455 (2007).
14. Naidu, P. D. & Malmgren, B. A. A high-resolution record of late Quaternary upwelling along the Oman Margin, Arabian Sea based on planktonic foraminifera. *Paleoceanography* **11**, 129–140 (1996).
15. Kutzbach, J. E. Monsoon climate of the Early Holocene: Climate experiment with the Earth's orbital parameters for 9000 years ago. *Science* **214**, 59–61 (1981).
16. Sun, Y., Clemens, S. C., An, Z. & Yu, Z. Astronomical timescale and palaeoclimatic implication of stacked 3.6-Myr monsoon records from the Chinese Loess Plateau. *Quat. Sci. Rev.* **25**, 33–48 (2006).
17. Clemens, S. C., Prell, W. L. & Sun, Y. Orbital-scale timing and mechanisms driving Late Pleistocene Indo-Asian summer monsoons: Reinterpreting cave speleothem  $\delta^{18}\text{O}$ . *Paleoceanography* **25**, PA4207 (2010).
18. Lewis, S. C., LeGrande, A. N., Kelley, M. & Schmidt, G. A. Water vapour source impacts on oxygen isotope variability in tropical precipitation during Heinrich events. *Clim. Past Discuss.* **6**, 87–133 (2010).
19. Turney, C. S. M. *et al.* Millennial and orbital variations of El Niño/Southern Oscillation and high-latitude climate in the last glacial period. *Nature* **428**, 306–310 (2004).
20. Muller, J. *et al.* Possible evidence for wet Heinrich phases in tropical NE Australia: The Lynch's Crater deposit. *Quat. Sci. Rev.* **27**, 468–475 (2008).
21. Kitoh, A. & Murakami, S. Tropical Pacific climate at the mid-Holocene and the Last Glacial Maximum simulated by a coupled ocean–atmosphere general circulation model. *Paleoceanography* **17**, 1047 (2002).
22. Zhang, R. & Delworth, T. L. Simulated tropical response to a substantial weakening of the Atlantic thermohaline circulation. *J. Clim.* **18**, 1853–1860 (2005).
23. Mohtadi, M. *et al.* Low-latitude control on seasonal and interannual changes in planktonic foraminiferal flux and shell geochemistry off south Java: A sediment trap study. *Paleoceanography* **24**, PA1201 (2009).
24. Qu, T., Du, Y., Strachan, J., Meyers, G. & Slingo, J. M. Sea surface temperature and its variability in the Indonesian region. *Oceanography* **18**, 50–62 (2005).
25. Grootes, P. M. & Stuiver, M. Oxygen 18/16 variability in Greenland snow and ice with  $10^{-3}$  to  $10^5$ -year time resolution. *J. Geophys. Res.* **102** No. C12, 26455–26470 (1997).
26. Wang, Y. *et al.* Millennial- and orbital-scale changes in the East Asian monsoon over the past 224,000 years. *Nature* **451**, 1090–1093 (2008).
27. Stenni, B. *et al.* A late-glacial high-resolution site and source temperature record derived from the EPICA Dome C isotope records (East Antarctica). *Earth Planet. Sci. Lett.* **217**, 183–195 (2004).

## Acknowledgements

We are grateful to M. Segl, B. Meyer-Schack, M. Klann, H. Buschhoff, V. Lukies and I. Meyer for technical support. This study was funded by the German Bundesministerium für Bildung und Forschung (PABESIA) and the Deutsche Forschungsgemeinschaft (DFG, HE 3412/15-1). D.W.O.'s participation was funded by the US National Science Foundation.

## Author contributions

M.M. was responsible for oxygen isotope analyses and *G. bulloides* counts, J.-B.W.S. was responsible for the grain-size data, R.D. and D.W.O. were responsible for the radiocarbon analyses, M.M. and S.S. were responsible for the X-ray fluorescence and lithogenic data, D.H. was chief investigator and A.L. was partner investigator, M.M., D.W.O. and S.S. wrote the paper; all the authors discussed the paper.

## Additional information

The authors declare no competing financial interests. Supplementary information accompanies this paper on [www.nature.com/naturegeoscience](http://www.nature.com/naturegeoscience). Reprints and permissions information is available online at <http://www.nature.com/reprints>. Correspondence and requests for materials should be addressed to M.M.